

doi: 10.15407/ujpe60.10.1055

A.B. SMIRNOV, A.A. KORCHOVYI, N.M. KROLEVEC, V.A. MOROZHENKO,  
R.K. SAVKINA, R.S. UDOVYTSKA, F.F. SIZOVV.E. Lashkaryov Institute of Semiconductor Physics, Nat. Acad. of Sci. of Ukraine  
(41, Nauky Ave., Kyiv 03028, Ukraine; e-mail: alex\_tenet@isp.kiev.ua)**STUDY OF THE MORPHOLOGY  
OF *p*-CdHgTe LAYERS STRUCTURED  
BY GRAZING SILVER-ION BEAM IRRADIATION**

PACS 61.72.uj

The “top-down” process of deposition of nanostructured layers on the surface of semiconductor materials by the ion implantation is studied. The irradiation of *p*-Cd<sub>x</sub>Hg<sub>1-x</sub>Te ( $x = 0.223$ )/CdZnTe heterostructures with 100-keV silver ions induces the formation of a nanostructure array on the specimen surface. The reduction of the ion beam incidence angle to 40° stimulates an ordering of nanostructures. The stabilization of the implantation-activated state of the system gives rise to the formation of the multifunctional metal oxide–semiconductor system Ag<sub>2</sub>O–*p*-Cd<sub>x</sub>Hg<sub>1-x</sub>Te ( $x = 0.2$ ). The latter is a size-dependent response to the grazing beam irradiation and allows the combination of the functional properties of Ag<sub>2</sub>O oxide ( $E_g = 1.41$  eV) and CdHgTe semiconductor ( $E_g = 0.123$  eV) to be used as a basis for the creation of optical transducers and microwave grid arrays.

*Keywords:* nanostructured layer, CdHgTe semiconductor, method of ion implantation.

**1. Introduction**

With diminishing the layout rules for integrated electronic devices, the cost of the lithographic equipment tends to an exponential growth, and lithography itself, although remaining an important technological stage at the creation of modern micro- and nanoelectronic devices, approaches the exhaustion of its potential. At the same time, the treatment of a semiconductor using concentrated fluxes of energy or particles is capable of forming a spectrum of useful topological features on its surface, such as a wavy nanorelief, terraces, hierarchical arrays of nanoobjects, and so forth. In particular, the powerful potential of the ionic bombardment allows regular structures about tens of nanometers in dimensions to be obtained with an accuracy comparable with the modern state of lithography [1–4].

For the first time, the formation of a wavy relief (“ripples”) on the surface of a condensed medium was detected in work [5], when treating a glass surface with the help of a wide beam of nitrogen ions from an atmospheric discharge. Considerable efforts were ap-

plied to study and interpret the microscopic dynamics of the process of structurization of the surfaces of metals, insulators, and semiconductors under the influence of the ionic bombardment [6, 7]. According to Bradley–Harper theoretical model [8, 9], the formation of ordered structures is a result of the instability induced by the dependence of sputtering coefficient on the distortion of a treated surface.

From the analysis of literature sources [10–15], it follows that the energy of ionic radiation provides a statistical description for the process of nanostructure formation. At the same time, the morphology and the structuring kinetics are dependent on the angle, at which the ionic flux interacts with the target surface. In our previous works [16–18], it was established that the irradiation of CdHgTe films by silver ions resulted in the nanostructuring of their surface and the formation of Ag<sub>2</sub>O in the matrix. This work is aimed at studying the character of changes in the structural properties of the narrow-gap semiconductor compound CdHgTe induced by a variation of the ionic irradiation angle and at analyzing a possibility of the controllable formation of the Ag<sub>2</sub>O–*p*-CdHgTe heterostructure on the surface. The ion-induced microstructuring in layers of the *p*-Cd<sub>x</sub>Hg<sub>1-x</sub>Te ( $x = 0.223$ ) solid solution will allow the functional prop-

© A.B. SMIRNOV, A.A. KORCHOVYI,  
N.M. KROLEVEC, V.A. MOROZHENKO,  
R.K. SAVKINA, R.S. UDOVYTSKA, F.F. SIZOV, 2015

ISSN 2071-0186. Ukr. J. Phys. 2015. Vol. 60, No. 10

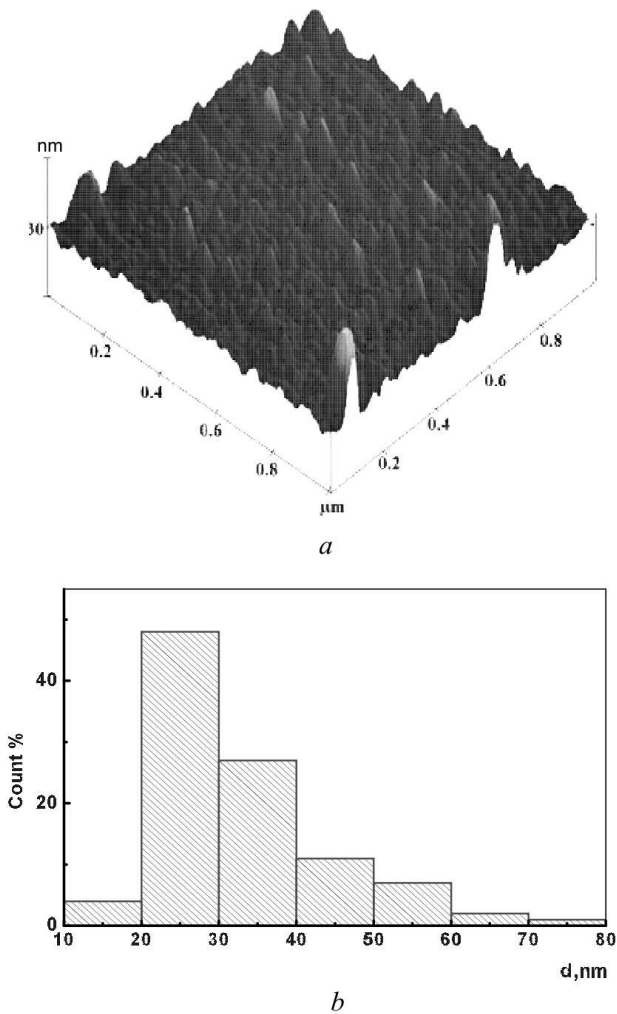


**Fig. 1.** AFM images of initial specimens of the  $p\text{-Cd}_x\text{Hg}_{1-x}\text{Te}$  ( $x = 0.223$ ) heteroepitaxial structure: the 3D image (a) and the size distribution histogram for particles located in the  $X\text{-}Y$  plane (b)

erties of  $\text{Ag}_2\text{O}$  oxide ( $E_g = 1.41$  eV) and  $\text{CdHgTe}$  semiconductor ( $E_g = 0.123$  eV) to be combined, which can become a basis for the creation of optical transducers and microwave grids.

## 2. Experimental Part

Heteroepitaxial films  $p\text{-Cd}_x\text{Hg}_{1-x}\text{Te}$  ( $x = 0.223$ ) on the  $\text{CdZnTe}$  substrate are experimentally studied. They were fabricated by the method of liquid-phase epitaxy and irradiated with 100-keV silver ions to an implantation dose of  $3 \times 10^{13}$   $\text{cm}^{-2}$  at room temperature. Silver ions were implanted both at the

normal beam incidence (to a double dose) and at an angle of  $40^\circ$  with respect to the specimen surface (to a single dose).

The surface of semiconductor films was researched in the contact regime within the AFM microscopy method (NanoScope IIIa Digital Instruments). In addition, the changes in the optical properties of heterostructures were studied by registering their transmission spectra.

## 3. Results

### 3.1. Topometry

In Figs. 1–3, a, the 3D AFM images for all studied specimens – initial, implanted at an angle of  $90^\circ$ , and implanted at an angle of  $40^\circ$ , respectively – are shown. The corresponding histograms for the size distribution of particles in the  $X\text{-}Y$  plane are depicted in Figs. 1–3, b. Table contains the surface parameters (the real surface area, the difference between the relief area and the ideal one, and the root-mean-square roughness) for the initial and implanted specimens of the  $\text{CdHgTe}$  heteroepitaxial structure.

The AFM images demonstrate a complicated relief of the heteroepitaxial film surface. The results of the initial specimen topometry (Fig. 1, a) show that the surface plane is densely and regularly packed with round shaped grains 20 to 40 nm in diameter. This means that the studied epitaxial film is characterized by a considerable nonequilibrium resource. As a rule, this state is concentrated in mechanical stresses of the local character (grains–pores), which is confirmed by the presence of a network of quasipores

### Parameters of the $\text{CdHgTe}$ surface before and after the implantation with silver ions

Specimen	Roughness parameters for a $1 \times 1\text{-}\mu\text{m}^2$ surface fragment		
	Real surface area, $\mu\text{m}^2$	Excess of relief area over ideal one, %	Root-mean-square roughness $R_q$ , nm
Initial	1.0375	3.75	3.34
Double implanted with silver at $90^\circ$	1.0093	0.93	2.17
Implanted with silver at $40^\circ$	1.03041	3.041	3.11

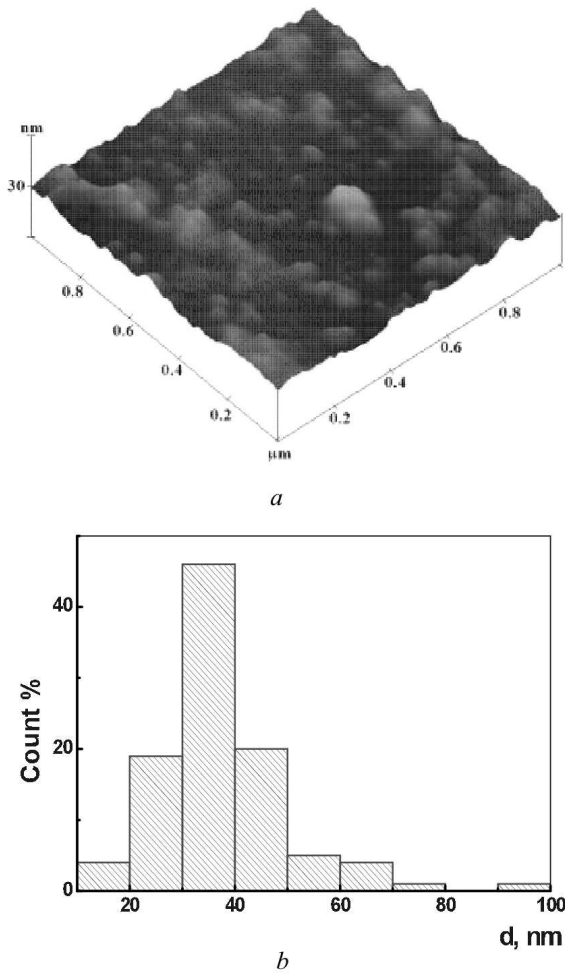


**Fig. 2.** The same as in Fig. 1, but for specimens irradiated with silver ions to the double dose at the normal ion incidence ( $90^\circ$ )

3.5–10 nm in depth and 50–160 nm in diameter. The root-mean-square roughness of a fragment of this surface amounts to 3.34 nm (see Table).

After the double implantation with silver ions at an angle of  $90^\circ$  (Fig. 2, *a*), the surface of the semiconductor film undergoes a transformation. The microrelief changes owing to the smearing of surface sections. The quaspores are almost unobservable, the grain boundaries are strongly smeared, and some grains, keeping their sizes invariable, form chains with channels between them. After the double implantation, the root-mean-square roughness reduced to 2.17 nm. There emerged a substantial discrepancy between the heights at different surface sections,

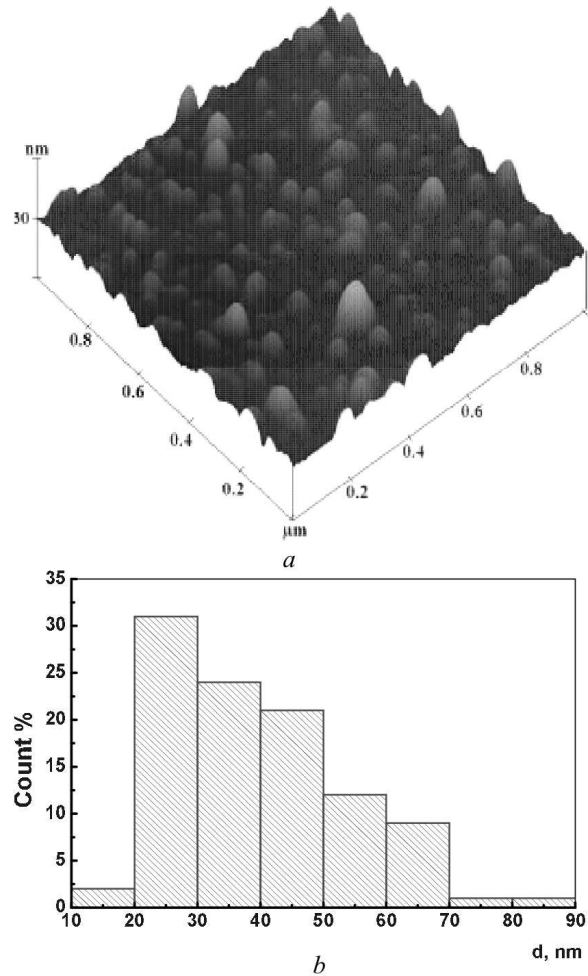


**Fig. 3.** The same as in Fig. 1, but for specimens irradiated with silver ions at an angle of  $40^\circ$  to the surface

which may probably be associated with the presence of the defect and defect-free semiconductor regions. Hence, the double implantation demonstrates the phenomenon of ionic sputtering and the degradation of the CdHgTe film surface.

After the implantation with silver ions at an angle of  $40^\circ$  with respect to the surface (Fig. 3, *a*), an insignificant growth of grain sizes to 60 nm was observed together with an insignificant smearing of grain boundaries of grains. The initial porosity remained the same at that. The relief became more developed. There emerged a uniform array of cone-shaped formations with the height  $h$  varying from 5 to 10 nm and the base diameter  $d$  from 50 to 80 nm. From Table, one can see that, after the im-

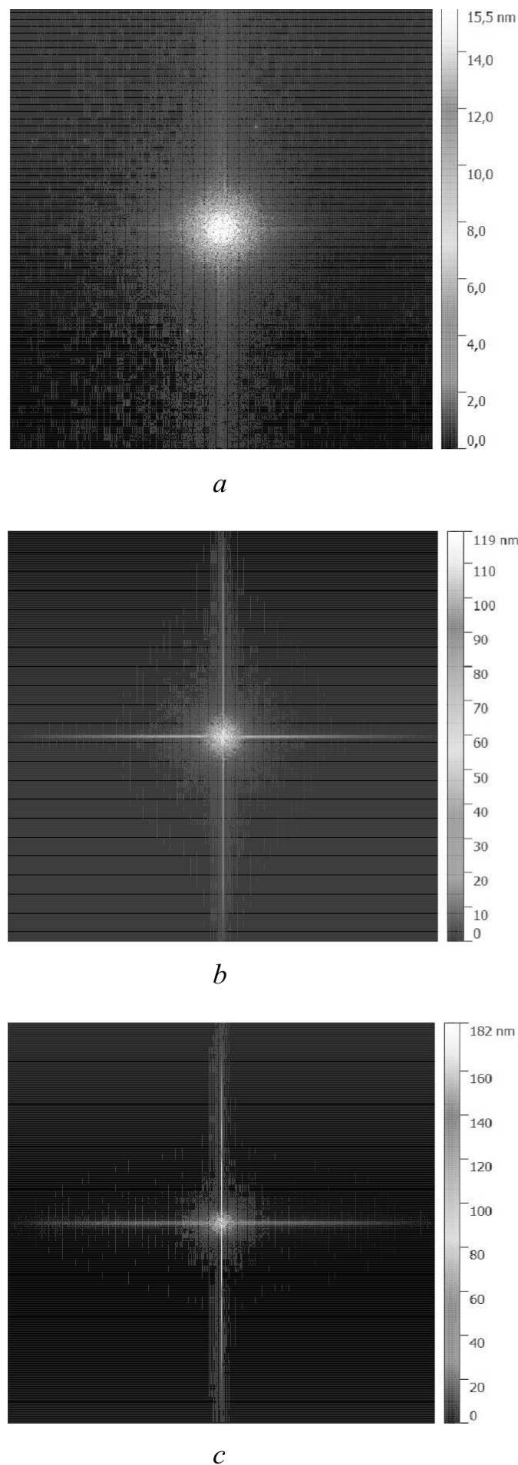


**Fig. 4.** Fourier transforms of AFM images obtained for various specimens: initial (a), implanted at a angle of  $40^\circ$  (b), and implanted to the double dose at an angle of  $90^\circ$  (c)

plantation with silver ions at an angle of  $40^\circ$ , the root-mean-square roughness decreased slightly (to 3.11 nm) in comparison with the initial value.

In order to determine the character of the size distribution for the objects localized on specimens' surface, the numerical processing of the obtained AFM images was carried out. As a result, we constructed the histograms which present the superposition of the distribution functions of lateral dimensions in the  $X - Y$  plane (see Figs. 1–3, b). The most probable size of nanoobjects was determined as the position of the major maximum in the distribution histogram.

The analysis of the size distribution functions for all specimens testifies to insignificant relative shifts of the major maxima (from 30 to 50%). Figure 1, b demonstrates that the size distribution of objects on the surface of the initial specimen is highly asymmetric, with the most probable grain size equal to 25 nm. The distribution histogram for the sizes of nanoobjects in CdHgTe films irradiated with an ionic beam at a normal angle to the specimen surface (Fig. 2, b) is symmetric with respect to the most probable size (35 nm). In other words, the distribution function of probable sizes shifts toward larger lateral dimensions in comparison with the initial specimen, and the distribution itself becomes more Gaussian-like. The size distribution histogram for nanoobjects on the specimen surface irradiated at an angle of  $40^\circ$  (Fig. 3, b) has a linear section (on the logarithmic scale). The presence of such a section means that the structures with a fractal geometry are formed on the surface of a semiconductor compound epitaxial film [19].

To verify the periodicity and the ordering in the systems concerned, the Fourier transforms were calculated for the AFM images of examined specimens (Fig. 4). For the initial specimen, the complete smearing of light boundaries is observed, and the Fourier transform has a diffusive character (Fig. 4, a). At the same time, the Fourier transform of the spatial frequencies on the CdHgTe surface structured by the ionic implantation testifies to the formation of a two-dimensional quasiperiodic bow-shaped structure from nanograins.

The Fourier transform shown in Fig. 4, b makes it possible to distinguish the ordered structures with the spatial periods  $1/f_1 = 80$  nm (the characteristic frequency  $f_1 = 1/80$  nm $^{-1}$ ) and  $1/f_2 = 90$  nm (the characteristic frequency  $f_2 = 1/90$  nm $^{-1}$ ). The

frequencies that form a “cross” at the center of frequency spectra (it is associated with the method of Fourier transformation) follow from the edge effect, and therefore they should be ignored. No characteristic frequencies for any periodic structures are observed in the Fourier transform of the AFM image for the specimen twice irradiated at an angle of  $90^\circ$  (Fig. 4, *c*). This fact testifies that the microscopic structure on the specimen surface was completely destroyed during the double-dose implantation.

### 3.2. Optical properties

The composition  $x$  and the homogeneity of epitaxial layers were estimated from their IR transmission spectra registered in the spectral interval of 2.5–20  $\mu\text{m}$  at room temperature. As one can see in Fig. 5, all specimens demonstrate a drastic transmittance reduction occurring at wavelengths  $\lambda < 9.9 \mu\text{m}$  and depending on the composition of the active CdHgTe layer ( $E_g = 0.123 \text{ eV}$ ). After the irradiation of specimens with silver ions, both normally (Fig. 5, curve 3) and at an angle of  $40^\circ$  with respect to the specimen surface (Fig. 5 curve 2), the growth of the optical transmittance is observed from an initial value of 40% to 50%, which agrees with the roughness decrease (see Table).

In the former case, the changes in the optical parameters can be associated with the smearing of sections on the CdHgTe heterostructure surface, which gives rise to the disappearance of the interference pattern in the Fourier spectra inherent to the substance in the initial state [20]. The more pronounced interference pattern obtained for the specimen irradiated at an angle of  $40^\circ$  may testify to a higher homogeneity of the layer across its thickness, which is in agreement with the effect of structure ordering, the reduction of pores, and the surface compaction, so that the interference in the transmission spectrum becomes more contrast, and the transmittance  $T$  increases (Fig. 5, curve 2).

For the specimen double-irradiated at an angle of  $90^\circ$ , in addition to the interference pattern smearing (Fig. 5, curve 3), one can observe a more drastic transmittance reduction, as the wavelength grows in the interval  $\lambda > 12 \mu\text{m}$ . In the interval  $h\nu < E_g$ , the absorption is known to occur at free charge carriers, which is responsible for the absorption coefficient dependences on the wavelength:  $\alpha(\lambda) \sim \lambda^2$  for *p*-CdHgTe and  $\alpha(\lambda) \sim \lambda^{3/2}$  for *n*-CdHgTe.

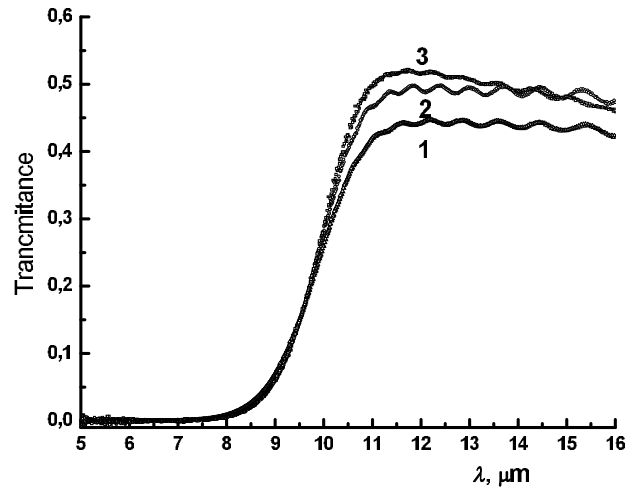


Fig. 5. Transmission spectra of various specimens: the initial (1), implanted at a angle of  $40^\circ$  (2), and implanted to the double dose at an angle of  $90^\circ$  (3)

Hence, in our case, the irradiation to the double dose could result in the transformation of the conductivity from the *p*- to *n*-type or in the formation of an *n*-CdHgTe layer. It should also be noted that since the optical transmittance depends not only on the absorption, but also on the reflection of light, the additional researches of optical and electrical properties of the irradiated material are required in order to unambiguously determine why  $T$  depends on  $\lambda$  more strongly.

### 4. Discussion

Hence, our research of the influence of the ionic bombardment on the structural properties of *p*-CdHgTe epitaxial films and its dependence on the ionic beam intensity and the incidence angle showed the following. The ionic irradiation of CdHgTe epitaxial films with silver ions at the normal ( $90^\circ$ ) ionic beam incidence on the surface of specimens gives rise to the formation of an array of nanostructures with lateral dimensions from 60 to 120 nm and heights from 12 to 16 nm [16, 17]. If the incidence angle of ion beam decreases down to  $40^\circ$ , the surface nanostructuring gets an ordered character: a two-dimensional quasiperiodic system with the spatial period  $1/f = 80 \div 90 \text{ nm}$  is formed. At the same time, the surface irradiation to the double dose at an angle of  $90^\circ$  results in a degradation of the CdHgTe film surface. It should be noted that the irradiation of CdHgTe films with boron ions

in the same experimental geometry (at the normal incidence of an ionic beam on the surface of specimens), with the same energy, and to the same dose as in the case with silver ions results in a surface damage that is substantially different by the character and the damaged layer thickness [16]. No nanostructuring of the surface is observed in that case. The character of CdHgTe crystal lattice distortions is also different: maximum mechanical stresses  $\sigma_{\max}$  in the damaged layer differ by two orders of magnitude, being similar to the squeezing in the case of boron ( $\sim 10^3$  Pa [16]), and the crystal lattice is stretched ( $\sim 10^5$  Pa [16]) at the implantation with larger ions ( $\text{Ag}^+$ ).

In our opinion, the complicated surface relief, which looks like an array of nanoislands, emerges due to the ion-beam erosion. This mechanism is relevant at the low-energy irradiation [9]. If a binary compound is irradiated, and either of its components is primarily sputtered, the compound stoichiometry becomes broken, and a layer with an alternative composition is formed on the material surface. The surface becomes enriched with heavier components of the Cd-HgTe solid solution such as Hg. This scenario agrees with the results of a X-ray diffraction analysis of Cd-HgTe films with the composition  $x = 0.23$  irradiated by 100-keV silver ions [18], which proved the formation of a CdHgTe polycrystalline layer with  $x = 0.2$  on the surface.

In addition, an important role in our case is played by the deformation induced by the ionic irradiation in the matrix. The difference between the effects that arise in the near-surface layer of a CdHgTe epitaxial film after its treatment with boron or silver ions stems from the opposite character of deformations generated by the ions in the crystal lattice of the semiconductor. In particular, the stretching deformations in the near-surface region of the  $p$ -CdHgTe epitaxial film and the compression of deeper layers stimulate the “withdrawal” of silver ions to the surface and the formation of the  $\text{Ag}_2\text{O}$  compound in the near-surface layer of the matrix (in accordance to data of the X-ray diffraction analysis reported in work [18]). The propensity of silver to create solid solutions in  $p$ -CdHgTe at the ionic implantation becomes a crucial factor.

In this work, the “top-down” process of nanostructured layer formation on the surface of a semiconductor material using the ion implantation technique was studied. The penetration of silver ions gave rise

to a modification of thermodynamic parameters in the damaged layer of the CdHgTe epitaxial film. The component stabilization in the nonequilibrium planar medium occurred through changes in the macro- and microscopic parameters of this complicated system. On the one hand, there emerged a stretching deformation, the energy of defect formation decreased, the crystal lattice parameters changed, the concentration and the diffusive mobility of defects increased, and so forth. On the other hand, the parameters of semiconductor planar microstructuring began to determine the state of the whole system. In this case, the stabilization of system’s state activated by the implantation gave rise to the formation of a polyfunctional metal oxide–semiconductor system  $\text{Ag}_2\text{O}-p\text{-Cd}_x\text{Hg}_{1-x}\text{Te}$ .

## 5. Conclusions

To summarize, the results of researches concerning the influence of the ionic bombardment on the structural properties of  $p$ -CdHgTe epitaxial films and its dependence on the ionic beam parameters are presented. The formation of nano-scaled surface structures on the film surface was demonstrated, and the structuring kinetics was shown to depend on the interaction angle between the ionic beam and the target surface. In the case of ionic irradiation of the target at an angle of  $40^\circ$ , the array of nanostructures with the lateral dimensions from 50 to 80 nm and the heights from 5 to 10 nm is formed on the specimen surface. The analysis of size distribution histograms obtained for nanoobjects on the surface of the specimen irradiated at an angle of  $40^\circ$  testifies to the formation of structures with a fractal geometry. The surface implantation of silver ions to the double dose at the normal ion-beam incidence results in a degradation of the CdHgTe film surface.

1. E. Chason and W.L. Chan, *Topics Appl. Phys.* **116**, 53. (2010).
2. B. Ziberi, M. Cornejo, F. Frost, and B. Rauschenbach, *J. Phys. Condens. Matter* **21**, 224003 (2009).
3. S. Facsco, T. Dekorsy, C. Koerdt, C. Trappe, H. Kurz, A. Vogt, and H.L. Hartnagel, *Science* **285**, 1551 (1999).
4. F. Frost, A. Schindler, and F. Bigl, *Phys. Rev. Lett.* **85**, 4116 (2000).
5. M. Navez, C. Sella, and D. Chaperot, *Acad. Sci. Paris* **254**, 240 (1962).

6. R. Cuerno and A.-L. Barabasi, Phys. Rev. Lett. **74**, 4746 (1995).
7. M. Makeev and A.-L. Barabasi, Appl. Phys. Lett. **71**, 2800 (1997).
8. R.M. Bradley and P.D. Shipman, Phys. Rev. Lett. **105**, 145501 (2010).
9. R.M. Bradley and J.M.E. Harper, J. Vac. Sci. Technol. A **6**, 2390 (1988).
10. P.A. Sigmund, J. Mater. Sci. **8**, 1545 (1973).
11. M. Castro, R. Cuerno, L. Vázquez, and R. Gago, Phys. Rev. Lett. **94**, 016102 (2005).
12. S. Facsko, T. Bobek, A. Stahl, and H. Kurz, Phys. Rev. B **69**, 153412 (2004).
13. M. Kardar, G. Parisi, and Y.C. Zhang, Phys. Rev. Lett. **56**, 889 (1986).
14. D.E. Wolf and J. Villian, Europhys. Lett. **13**, 389 (1990).
15. Y. Kuramoto and T. Tsuzuki, Prog. Theor. Phys. **55**, 356 (1976).
16. A.B. Smirnov, O.S. Litvin, V.O. Morozhenko, R.K. Savkina, M.I. Smoliy, R.S. Udovyt'ska, and F.F. Sizov, Ukr. J. Phys. **58**, 872 (2013).
17. Patent of Ukraine for useful model, No. 87886, 25.02.2014.
18. F.F. Sizov, R.K. Savkina, A.B. Smirnov, R.S. Udovyt'ska, V.P. Kladko, A.I. Gudimenko, N.V. Safruk, and O.S. Lytvyn, Phys. Solid State **56**, 2160 (2014).
19. A.-L. Barabasi and H.E. Stanley, *Fractal Concepts in Surface Growth* (Cambridge Univ. Press, Cambridge, 1995).
20. A.V. Nikonov, K.O. Boltar, and N.I. Iakovleva, Usp. Prikl. Fiz. **1**, 500 (2013).
21. Li Biao, J.H. Chu, Z.H. Chen, Y. Chang, H.M. Ji, and D.Y. Tang, J. Appl. Phys. **79**, 7738 (1996).

Received 20.01.15.

Translated from Ukrainian by O.I. Voitenko

*О.Б. Смирнов, А.А. Корчовий,  
М.М. Кролевець, В.О. Мороженко,  
Р.К. Савкіна, Р.С. Удовіцька, Ф.Ф. Сизов*

ДОСЛІДЖЕННЯ МОРФОЛОГІЇ ШАРІВ  
*p*-CdHgTe СТРУКТУРОВАНИХ КОВЗНИМ  
ОПРОМІНЕННЯМ ІОНАМИ СРІБЛА

Резюме

У роботі вивчається “top-down” процес отримання наноструктурованого шару на поверхні напівпровідникового матеріалу методом іонної імплантації. У результаті опромінення гетероструктур *p*-Cd<sub>*x*</sub>Hg<sub>1-*x*</sub>Te (*x* = 0,223)/CdZnTe іонами срібла з енергією 100 еВ на поверхні зразків відбувається утворення масиву наноструктур. Зменшення кута падіння іонного пучка до 40° приводить до того, що наноструктурування набуває впорядкованого характеру. При цьому наслідком стабілізації активованого імплантацією стану системи є утворення поліфункціональної системи оксид металу-напівпровідник Ag<sub>2</sub>O-*p*-Cd<sub>*x*</sub>Hg<sub>1-*x*</sub>Te (*x* = 0,2), що є розмірно-залежним відгуком на опромінення ковзним опроміненням та, що дозволяє сумістити функціональні властивості оксиду Ag<sub>2</sub>O (*E<sub>g</sub>* = 1,41 еВ) та напівпровідника CdHgTe (*E<sub>g</sub>* = 0,123 еВ), як основи для створення оптичних перетворювачів та масивів з НВЧ ґраток.